JOURNAL OF QUATERNARY SCIENCE (2013) **28**(4) 349–359 ISSN 0267-8179. DOI: 10.1002/jqs.2625

Palaeoenvironmental implications of evaporative gaylussite crystals from Lonar Lake, central India

A. ANOOP,[1,2] S. PRASAD,[1]* B. PLESSEN,[1] N. BASAVAIAH,[3] B. GAYE,[4] R. NAUMANN,[1] P. MENZEL,[4] S. WEISE[5] and A. BRAUER[1]

[1]German Research Center for Geosciences (GFZ), Section 5.2, Climate Dynamics and Landscape Evolution, Telegrafenberg, D-14473, Potsdam, Germany
[2]DFG Graduate School 1364, University of Potsdam, Germany
[3]Indian Institute of Geomagnetism, Navi Mumbai, India
[4]Universität Hamburg, Institute of Biogeochemistry and Marine Chemistry, Hamburg, Germany
[5]UFZ Centre for Environmental Research, Department of Catchment Hydrology, Halle, Germany

Received 23 March 2012; Revised 11 January 2013; Accepted 13 January 2013

ABSTRACT: We have undertaken petrographic, mineralogical, geochemical and isotopic investigations on carbonate minerals found within a 10-m-long core from Lonar Lake, central India, with the aim of evaluating their potential as palaeoenvironmental proxies. The core encompasses the entire Holocene and is the first well-dated high-resolution record from central India. While calcite and/or aragonite were found throughout the core, the mineral gaylussite was found only in two specific intervals (4630–3890 and 2040–560 cal a BP). Hydrochemical and isotope data from inflowing streams and lake waters indicate that evaporitic processes play a dominant role in the precipitation of carbonates within this lake. Isotopic ($\delta^{18}O$ and $\delta^{13}C$) studies on the evaporative gaylussite crystals and residual bulk carbonates (calcite) from the long core show that evaporation is the major control on $\delta^{18}O$ enrichment in both the minerals. However, in case of $\delta^{13}C$ additional mechanisms, for example methanogenesis (gaylussite) and phytoplankton productivity (calcium carbonate), play an additional important role in some intervals. We also discuss the relevance of our investigation for palaeoclimate reconstruction and late Holocene monsoon variability. Copyright © 2013 John Wiley & Sons, Ltd.

KEYWORDS: evaporites; gaylussite; isotopes; Lonar Lake; monsoon.

Introduction

The mineralogy and geochemistry of lacustrine carbonates are widely used to infer palaeoenvironmental changes (Stuiver, 1970; Drummond *et al.*, 1995; Leng and Marshall, 2004; Mangili *et al.*, 2010). Fluctuations in the isotope composition ($\delta^{18}O$ and $\delta^{13}C$) of authigenic carbonate minerals can be used to infer long-term changes in the precipitation/evaporation (P/E) ratio, temperature, photosynthetic pathways, changes in seasonality, and amount and tracks of precipitation (Leng *et al.*, 2006; Spötl *et al.*, 2010). The fundamental assumption underlying such investigations is the primary, unaltered nature of the carbonates, as isotopic exchange with interstitial brines, re-precipitation and/or re-crystallization can result in the loss of primary signals (Pendall *et al.*, 1994). In this study we present the results of our investigations on carbonates found in a 10-m-long sediment core, encompassing the Holocene, raised from the Lonar Lake in central India.

Lonar, an impact crater lake (Fredriksson *et al.*, 1973; Milton *et al.*, 1975; Maloof *et al.*, 2009), is located in the core monsoon zone (CMZ) of central India. The available evidence indicates that the Indian summer monsoon (ISM) remained the dominant precipitation source in this region during the Holocene (Prasad and Negendank, 2004). Central India is a climatically sensitive region as the interannual variability of the ISM in the CMZ is strongly correlated with the all India monsoon rainfall (Rajeevan *et al.*, 2010) and is impacted by various teleconnections (El Niño-Southern Oscillation, Indian Ocean Dipole, tropical mid-latitude interactions) (Krishnan *et al.*, 2000; Gadgil, 2003; Ashok *et al.*, 2004). Lonar Lake offers the rare possibility of undertaking a long-term regional palaeoclimate reconstruction as most of central India is covered by the Deccan basalts and lacks natural lakes.

Investigations on Lonar sediment cores revealed abundant gaylussite crystals ($Na_2CO_3 \cdot CaCO_3.5H_2O$) in some sections – the first such discovery from the Indian subcontinent. The primary gaylussite mineral is mostly precipitated by the gradual evaporative concentration of the brine (Hardie and Eugster, 1970; Eugster and Hardie, 1978; Mees *et al.*, 1991) at the sediment–water interface (Bischoff *et al.*, 1991) in contrast to calcite and aragonite that form in surface waters (McConnaughey *et al.*, 1994; Leng and Marshall, 2004; Reddy and Hoch, 2011). Gaylussite usually succeeds the precipitation of calcite and is the first sodium carbonate mineral to be precipitated when saline, alkaline waters are concentrated by evaporation (Rankama and Sahama, 1964; Renaut *et al.*, 1986). Simulated evaporative concentration of brine after the precipitation of gaylussite eventually leads to the precipitation of trona (Na_3H $(CO_3)_2.2H_2O$) (Hardie and Eugster, 1970; Eugster and Hardie, 1978). However, gaylussite can also form by secondary processes when alkaline brine rich in sodium reacts with (i) primary calcite aragonite; (ii) waters containing Ca^{2+} and HCO_3^-; or (iii) calcite-rich sediments (Eugster and Hardie, 1978). Due to its rare occurrence in nature (e.g. Eugster and Hardie, 1978; Renaut *et al.*, 1986; Bischoff *et al.*, 1991; Mees *et al.*, 1991; Partridge *et al.*, 1993), only one study (Mees *et al.*, 1998) has as yet investigated the potential of isotope data from gaylussite for palaeoclimate reconstruction.

The objectives of the present study were to: (i) examine the evidence for primary versus diagenetic origin of gaylussite crystals; (ii) investigate possible factors influencing the formation of carbonates in Lonar Lake, namely stream water chemistry and/or salinity induced by changes in input (inflow + precipitation)/evaporation; (iii) evaluate the feasibility of using carbonate mineralogy and isotopic composition of gaylussite

*Correspondence: S. Prasad, as above.
E-mail: sushma.prasad@gfz-potsdam.de

as an indicator of past hydrological changes; (iv) assess if isotopic investigations on gaylussite offer any additional environmental information compared with isotope data from calcite and/or aragonite.

Study site

Lonar Lake is situated in the village Lonar, Buldhana district of Maharashtra State, India (19°58′N, 76°30′E; 600 m a.s.l) in Deccan flood basalts (Fig. 1a). Based on previous geological studies, it is postulated that the lake was formed as a result of meteorite impact about 570 ka BP on the ~65 Ma old basalt flows of the Deccan Traps (Jourdan *et al.*, 2011). The impact crater is a near-circular depression with a 1.8-km rim-to-rim diameter, and ~1.4 km of lithic breccias ejecta around the crater rim. The ejecta cover an area of ~ 6.7 km^2 and extend to a distance of ~ 700 m in all directions from the crater rim except to the west where it extends to a distance of more than 1 km (Misra *et al.*, 2010). The crater has a raised rim of about 30 m from the surrounding plains due to uplift of the target layers and deposition of ejected debris, and a depth of around 135 m from the rim crest to the crater floor (La Touche and Christie, 1912; Fudali *et al.*, 1980). The crater walls exhibit steep slopes, with the inner rim averaging 30° in the west and south-west and 15–18° in the east. A network of rills and gullies is formed on the walls of the crater due to intermittent runoff erosion. The Quaternary deposits found within the crater consist of gravel to boulder talus which accumulated below the upper sparsely vegetated slopes of the inner crater. Additionally, palaeosols, termed as 'red bole beds', formed by the weathering of lava flows are also reported within the inner crater (Naidu *et al.*, 1990; Maloof *et al.*, 2009).

Modern climate and hydrology

The modern-day rainfall in the Lonar region is mostly provided by the Arabian Sea branch of the south-west monsoon (Sengupta and Sarkar, 2006). The wet and dry seasons of the monsoon system, along with the annual temperature fluctuations, produce three general climatic periods: (i) hot, wet weather from June to the end of September (southwest monsoon) with an average rainfall of 680 mm; (ii) cool and dry conditions from early October to February; and (iii) hot, dry weather from March to June. Temperatures during the pre-monsoon period are around 31 °C, but may increase up to 45 °C; southwest monsoon and post-monsoon temperatures average 27 and 23 °C, respectively.

Lonar Lake is a hyposaline (Jhingran and Rao, 1958; Nandy and Deo, 1961), alkaline lake (Joshi *et al.*, 2008) with a maximum depth of less than 7 m. The lake is stratified throughout the year with anoxic bottom waters below 43 m depth. The pH of Lonar Lake water varies from 9.2 to 10.5 with maximum during the pre-monsoon season (Borul, 2012). The salinity of lake water fluctuates between 7600 and 5600 mg L^{-1} with maximum during the pre-monsoon season and minima in the monsoon period (Pawar, 2010). The lake is mostly fed by ephemeral runoff during the southwest monsoon and three groundwater-fed perennial streams which originate from a gully in the north-east (Dhara and Sitanahani) and from the foot of the eastern crater wall (Ramgaya) (Fig. 1b). The lake can be regarded as a closed hydrological system owing to the absence of surface outlets. The absence of outflowing streams results in seasonal lake level fluctuations in response to regional climate patterns. During the summer monsoon (June to September) precipitation is very high and equals or even exceeds evapotranspiration. This leads to significant (*c.* 2 m) lake level rise for the period of summer monsoon accompanied by dilution-imposed changes in chemical composition of the lake water (Badve *et al.*, 1993). However, during dry seasons with low or absent precipitation, evaporation exceeds precipitation, leading to increased salt concentration in the surface waters (Badve *et al.*, 1993).

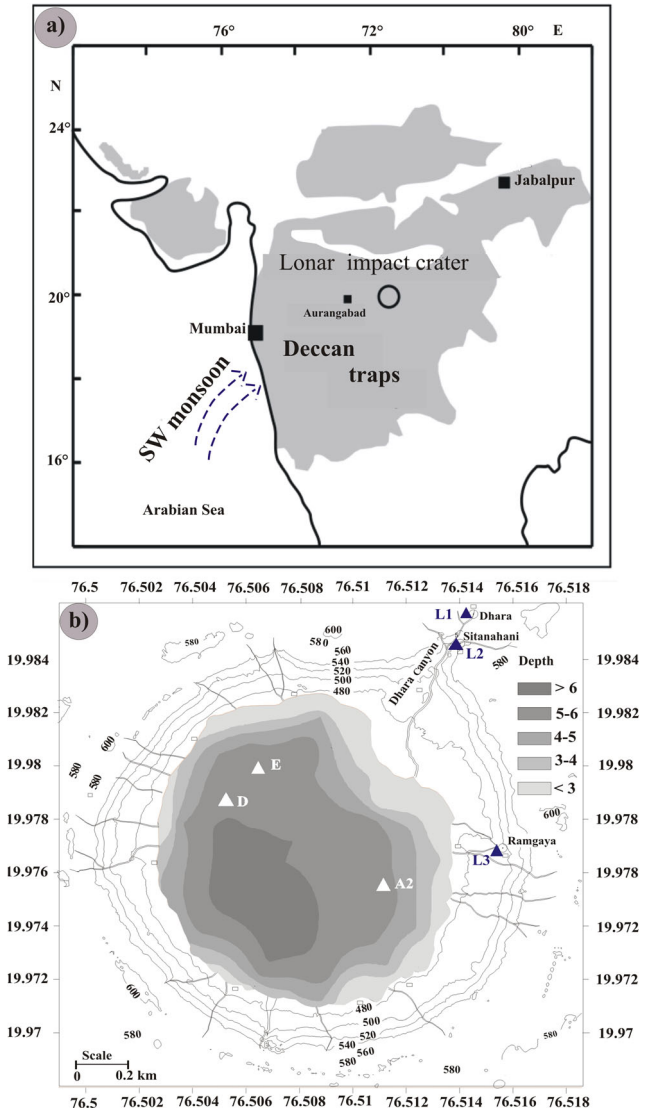

Figure 1. (a) Location of Lonar impact crater on the 65 Ma old Deccan Trap basalt (after Chakrabarti and Basu, 2006). (b) Crater contours (Maloof *et al.*, 2009), bathymetry of Lonar Lake and location of sampled lake water (white triangles) and inflowing streams (black triangles) for hydrochemistry and isotopic composition.

Methods

Sampling

In May–June 2008 we retrieved a 10-m composite core from the Lonar Lake at a water depth of 5.4 m using a UWITEC Sediment Piston corer. Lake water samples were collected from the oxic (*c.* 50 cm) and anoxic bottom layer (*c.* 400 cm) in February 2011. The samples were filtered through Whatman cellulose acetate membrane filters (pore size 0.45 μm), filled into pre-washed polyethylene bottles and stored in a refrigerator prior to analysis in the laboratory. For cation analysis, some drops of concentrated nitric acid were added to the filtered samples to lower the pH to 2–3.

Analytical procedure

X-ray diffraction (XRD) and thin sections studies were used for the determination of the carbonate mineral assemblages within the core sediments. The XRD analyses were performed using a Bruker-axs D5000 analytical system with measurements done at an angular range of 4–75°2θ with CuKα radiation. Additionally, quantitative determination of the chemical compositions of the gaylussite crystals was carried out using X-ray fluorescence (XRF). For this, 1 g powdered sample was mixed together with 6 g Fluxana and 0.5 g nitrate ammonium and gradually heated on five different burners. The resulting glass discs were analysed for chemical composition using a PANalytical AXIOS Advanced analytical system.

Stable isotope analysis ($\delta^{13}C_{gy}$ and $\delta^{18}O_{gy}$) of the gaylussite crystals was performed at 0.5–4 cm (*c.* 3–20 years) resolution. The crystals found within the sediments were handpicked under the microscope. As gaylussite crystals are known for their high solubility (Buchardt *et al.*, 2001), isotope analysis of crystals from the same depth (dry cleaned under the microscope or washed) was carried out to detect any possible changes in the isotope values due to washing with water. The results obtained show constant values for all the analyses. Therefore, all crystals were cleaned with distilled water prior to the analysis.

For isotopic analysis, small parts (about 50 μg) of the cleaned gaylussite crystals were weighed into glass vials. The stable isotope measurements were made using an automated carbonate extraction system (KIEL-IV) interfaced with a MAT253 IRMS (Isotope Ratio Mass Spectrometry). Isotopic ratios relative to the VPDB (Vienna Peedee Belemnite) are calibrated to NBS19 (limestone) with a precision better than 0.03‰ for $\delta^{13}C$ and 0.06‰ for $\delta^{18}O$ measurements. No data are available on the fractionation factors of sodium-bearing carbonates, and therefore no quantitative estimates can be made with our data.

The stable isotope ($\delta^{13}C_{bulk}$ and $\delta^{18}O_{bulk}$) compositions of bulk carbonates (calcite and/or aragonite) were determined in continuous flow mode using a Finningan GasBenchII with a carbonate option coupled to a DELTAplusXL mass spectrometer. The gaylussite crystals handpicked under the microscope were removed from the samples prior to analyses. From each sample, about 400 μg was loaded into 10-mL Labco Exetainer vials. After automatically flushing with He, the carbonate samples were reacted with phosphoric acid (100%) at 75 °C for 60 min, following the analytical procedure described by Spötl and Vennemann (2003). The isotope compositions were given relative to the VPDB standard in the conventional delta notation, and were calibrated against two international reference standards (NBS19 and NBS18). The standard deviation (1 sigma) for reference analyses was 0.06‰ for $\delta^{13}C$ and 0.08‰ for $\delta^{18}O$.

For total carbon and nitrogen determination, around 25 mg of powdered sample was loaded in tin capsules and combusted in the elemental analyser. Total carbon and nitrogen content were calibrated against acetanilide whereas for the nitrogen isotopic composition two ammonium sulphate standards (e.g. IAEA N-1 and N-2) were used. Replicate determinations show a standard deviation better than 0.2% for C and N.

$\delta^{13}C_{org}$ measurements of the bulk samples were performed using *in-situ* decalcified samples measured with elemental analyser (NC2500 Carlo Erba) coupled via a ConFlowIII interface to a DELTA^{plus}XL mass spectrometer. Around 3 mg of sample was weighted into silver capsules, treated with 20% HCl, heated for 3 h at 75 °C, and finally wrapped within the silver capsules and measured as described above. The calibration was performed using elemental (Urea) and certified isotope standards (USGS24, IAEA_CH-7) and proven with an internal soil reference sample (Boden3). The reproducibility for replicate analyses was 0.2‰ for $\delta^{13}C_{org}$.

For analysis of stable isotopes of water ($\delta^{2}H_{H2O}$ and $\delta^{18}O_{H2O}$), a few millilitres was filtered and filled into vials for automated analyses by cavity ring-down spectroscopy (Picarro L2120i with PAL autosampler and high-accuracy vaporizer). For every run the common data range was calibrated by two standards and additionally checked by a procedural standard. The analytical range of uncertainty was 0.25‰ ($\delta^{18}O_{H2O}$) and 0.8‰ ($\delta^{2}H_{H2O}$), respectively. In a ThermoFinnigan GasBench II the dissolved inorganic carbon (DIC) from water samples is converted with orthophosphoric acid to CO_{2DIC}, which is flushed with a helium carrier to a Conflow III-DELTA Vplus mass spectrometer system determining its $\delta^{13}C_{DIC}$. The data were calibrated in an manner analogous to that for $\delta^{2}H_{DIC}$ and $\delta^{18}O$ and the analytical range of uncertainty for $\delta^{13}C_{DIC}$ was ± 0.3‰.

Chronology

The chronology of the Lonar Lake core sediments was derived from 18 ^{14}C dates obtained from wood, leaf, bulk organic material and gaylussite crystals. Radiocarbon dating was carried out at Poznan radiocarbon laboratory, Poland. The ^{14}C dates obtained were calibrated using OxCal 4.1 software (Bronk Ramsay, 2008, 2009) with the IntCal 09 calibration curve (Reimer *et al.*, 2009).

Results

Modern hydrochemical data

The hydrochemistry of Lonar Lake water shows high values, varying between 3750 ± 330 and 3850 ± 370 mg L^{-1}, for Cl^- anions and Na^+ cations, respectively (Table 1). An increase in Na^+ and Cl^- ion concentrations is seen towards the anoxic bottom waters. The Cl^- and Na^+ ion concentrations from the

Table 1. Hydrochemistry and isotope data of Lonar Lake water and inflowing streams. Note that O-LW represents oxic lake water and A-LW denotes anoxic lake water.

No.	Type	Lat. (°N)	Long. (°E)	Na (mg L^{-1})	Cl (mg L^{-1})	K (mg L^{-1})	Mg (mg L^{-1})	Ca (mg L^{-1})	$\delta^{18}O$ (‰)	δD (‰)	$\delta^{13}C_{DIC}$ (‰)
A2	O-LW	19.976	76.511	3487	3423	9	31	n.a.	4.20	14.7	12.9
A2	A-LW	19.976	76.511	3776	3424	9	13	n.a.	4.30	15.3	12.0
D	O-LW	19.979	76.505	3795	3464	16	70	19	4.40	16.1	13.0
D	A-LW	19.979	76.505	3897	3494	10	74	n.a.	4.30	15.6	11.9
E	O-LW	19.980	76.507	3800	3996	12	88	n.a.	4.40	16.4	11.5
E	A-LW	19.980	76.507	4322	4079	15	12	n.a.	5.50	21.0	14.8
L1	Spring	19.986	76.514	58	97	2	59	72	−2.40	−15.4	−12.6
L2	Spring	19.985	76.514	45	24	1	36	30	−3.10	−21.3	−11.9
L3	Spring	19.977	76.515	73	59	1	47	43	−2.00	−13.0	−9.9

inflowing streams show low values of 59–97 and 32–73 mg L^{-1} respectively. Other major cations (K^+ and Mg^{2+}) in the lake water show substantially lower values varying between 9–14 and 9–88 mg L^{-1}, respectively. The Ca^{2+} concentrations in the measured lake water samples are below the detection limit while the values from the inflowing streams vary between 42 and 72 mg L^{-1}.

Isotope data ($\delta^{18}O$, δD and $\delta^{13}C_{DIC}$) of lake waters and inflowing streams are listed in Table 1. The $\delta^{18}O$ and δD of the inflowing streams range from −2.1 to −3.1‰ and −15.4 to −21.4‰, respectively. However, the lake water samples show relatively high values for $\delta^{18}O$ and δD isotopes, fluctuating between +4.2 to +5.5‰ and +14.7 to +21‰, respectively. Similarly, $\delta^{13}C_{DIC}$ is relatively high (+11 to +14.8‰) for the lake water samples and low for the inflowing streams (−9.9 to −12.6‰).

Carbonate precipitation

Samples from a thick efflorescent mineral crust (collected from the local villagers) formed in AD 1982 when the lake completely dried up were investigated to understand the modern-day mineral precipitation during extreme salinity conditions. The crusts were dry and porous comprising circular to elongate vugs, up to several millimetres wide, containing crystals (Fig. 2a). XRD analysis of these efflorescent crusts and the crystals revealed that they are not composed of equilibrium assemblages but dominated by a single mineral trona. The stable isotope analyses performed on these trona crystals yielded values of 8.3 and 8.5‰ for $\delta^{18}O$ and 7.4 and 8‰ for $\delta^{13}C$. This thick crust was dissolved during the following monsoon season. The calcite in surface sediments shows less enriched values near the stream inflow ($\delta^{13}C = -4.06$‰, $\delta^{18}O = -3.22$‰) as compared to deeper water ($\delta^{13}C = 4.46$‰, $\delta^{18}O = 0.95$‰) due to the dilution effect by the inflowing streams.

Carbonate distribution

Detailed petrographic analysis combined with XRD analyses shows that the carbonate in the core consists of calcite and aragonite in mineral phase and gaylussite occurring as crystals (Fig. 2b). There is a noticeable difference in the vertical distribution of carbonate minerals within the core (Fig. 3a,b). Calcite is the major carbonate mineral found in the entire core. Aragonite is restricted to the core interval between ca. 8.2 and 8.5 m (ca. 7200–5150 cal a BP) whereas gaylussite crystals (Fig. 2b) are found in two distinct zones at 1.58–4.22 m (2040–560 cal a BP, upper zone) and 6.42–7.6 m (4630–3890 cal a BP, lower zone) (Fig. 3a). Therefore, a sequential deposition of carbonate minerals occurs within the core, with precipitation of Ca carbonates (aragonite/calcite) followed by coexistence of Ca carbonates (calcite) and Na–Ca carbonates (gaylussite) and even exclusive occurrences of gaylussite crystals (Fig. 3b).

Gaylussite crystals

Microfacies and mineralogy

The gaylussite-bearing horizons are characterized as graded, with larger crystals at the base and a fining of the crystal size towards the top. They range in length from submillimetre to 10 mm, with smaller crystals showing higher crystallanity (euhedral forms) than the larger crystals. Most of the crystals appear parallel to the original sediment laminations. With a few exceptions, the crystals are devoid of any sediment inclusions. Quantitative chemical analyses of the gaylussite crystals reveal oxide percentages (± 0.2%) of CaO = 19.05%, Na_2O = 20.47%, H_2O = 30.3% and CO_2 = 29.4%. No other major components are present above 0.1 wt%.

Isotope ($\delta^{18}O_{gy}$ and $\delta^{13}C_{gy}$) analysis of gaylussite crystals

Lower gaylussite zone (G1: 4630–3890 cal a BP)

The stable isotope analyses on the lower gaylussite zone yielded high values for $\delta^{18}O_{gy}$ and $\delta^{13}C_{gy}$ ranging between +10 to +16‰ and +13 to +20‰, respectively. The most striking feature of the $\delta^{18}O_{gy}$ and $\delta^{13}C_{gy}$ isotopic values are their strong positive correlation ($r = 0.89$, significant at 99% confidence level) (Fig. 4a). The isotopic values show a progressive enrichment with decreasing age (see Fig. 6).

Upper gaylussite zone (G2: 2040–560 cal a BP)

The upper gaylussite zone also yielded high values of +8 to +18‰ and +9 to +15‰ for $\delta^{18}O_{gy}$ and $\delta^{13}C_{gy}$, respectively. A progressive enrichment in both isotopes is seen until ca. 1450 cal a BP. Subsequently, while $\delta^{18}O_{gy}$ continues with its enrichment trend, $\delta^{13}C_{gy}$ shows a stable or a depleting trend (see Fig. 6). The drop in the $\delta^{13}C_{gy}$ resulted in the formation of two distinct subzones within the upper gaylussite zone (2040–1450 and 1450–560 cal a BP) with correlation coefficients of $r = 0.68$ and −0.41, respectively (both significant at 95% confidence level) (Fig. 4b).

Isotope data on bulk carbonates ($\delta^{18}O_{bulk}$ and $\delta^{13}C_{bulk}$)

The stable isotope composition of bulk carbonates (without visible gaylussite) in the G1 zone ranges from −11.3 to +6.7‰

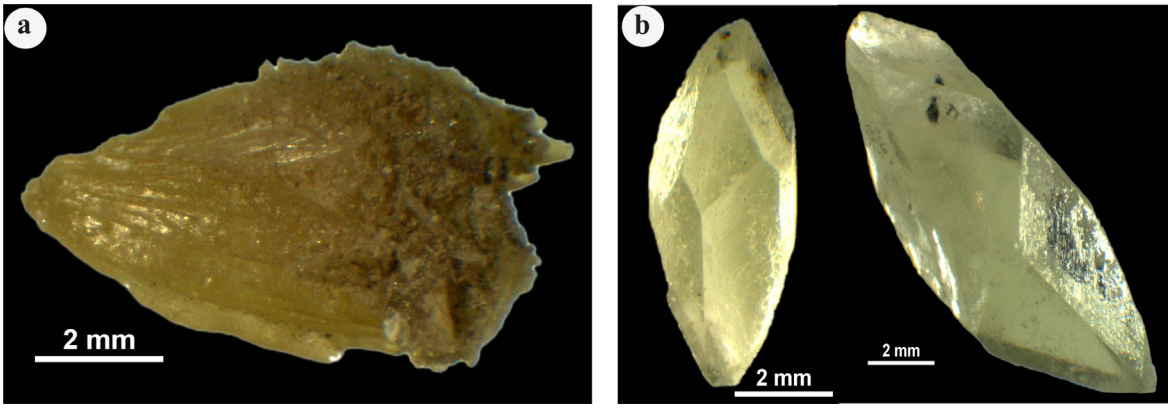

Figure 2. (a) Trona found in Lonar Lake (modern environment) when the lake was completely dried up in 1982 AD. (b) Gaylussite crystals found within the lake sediments. (Color figure can be seen in the online version of this article, available at http://wileyonlinelibrary.com/journal/jqs)

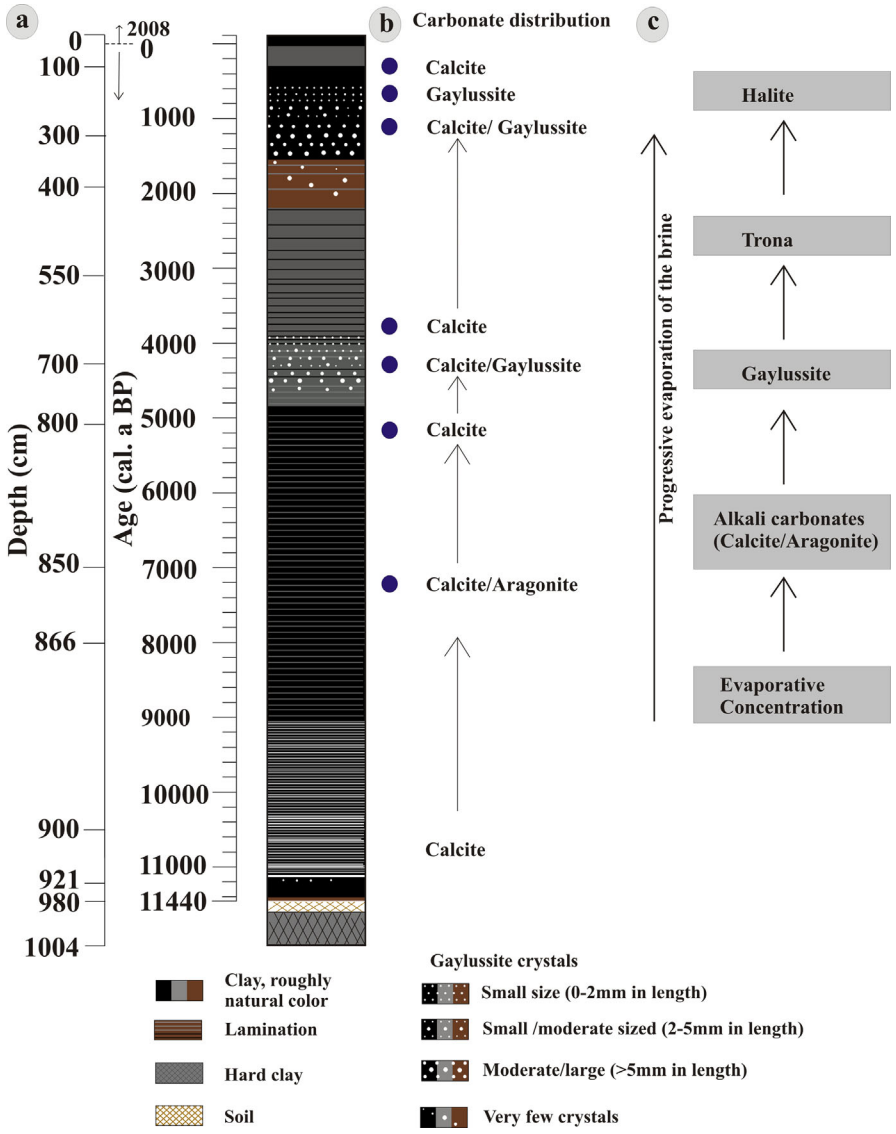

Figure 3. (a) Lithology of the Lonar core. b) Carbonate distribution within the core sediments. c) Sequential evaporative precipitation of minerals (modified after Hardie and Eugster, 1970; Eugster and Hardie, 1978). (Color figure can be seen in the online version of this article, available at http://wileyonlinelibrary.com/journal/jqs)

for $\delta^{18}O_{bulk}$, and −3.7 to +14‰ for $\delta^{13}C_{bulk}$. The $\delta^{18}O_{bulk}$ and $\delta^{13}C_{bulk}$ values show a strong positive correlation coefficient of 0.85 (significant at 99% confidence level) (Fig. 5a).

In the upper zone (G2) bulk carbonates range from −11.2 to +8.1‰ for $\delta^{18}O_{bulk}$, and −2 to +12‰ for $\delta^{13}C_{bulk}$. A strong positive correlation of 0.79 similar to the G1 zone is noted for the bulk carbonate values (Fig. 5b). However, unlike the lower zone a persistent stable enriched trend was noted for the $\delta^{18}O_{bulk}$ and $\delta^{13}C_{bulk}$ values after ca. 1450 cal a BP (Fig. 6).

Isotope and C/N data on bulk organic matter

$\delta^{13}C_{org}$ of the bulk sediment in the lower gaylussite (G1) zone shows values between −10.6 and −21‰ with a slight depleting trend. The C/N values for most of the G1 zone shows values (>20) indicative of the dominant terrestrial vegetation contribution. However, a sharp drop in C/N values (≤15) was noticed between ca. 4450 and 4300 cal a BP. In the upper gaylussite (G2) zone $\delta^{13}C_{org}$ varies between −18.9 and −12.8‰. The values show no particular trend until ca. 1450 cal a BP when an enrichment trend (up to 5‰) is noticed for ca. 100 years followed by a relatively high stable value (Fig. 6). Similarly, C/N values show a sudden persistent shift to aquatic-dominated values (≤15) around 1450 cal a BP (Fig. 6).

Discussion

Evidence for primary versus diagenetic origin of gaylussite

Gaylussite crystals in Lonar core sediments occur within distinct zones at 1.58–4.22 m and 6.42–7.6 m depth, implying that they were formed when the water chemistry was conducive for their formation. The crystals are parallel to the original sediment lamination and, with a few exceptions, free from sediment inclusions, indicating a synsedimentary origin. The stratigraphic variation in the distribution of the carbonate minerals also provides useful insights into the formation of evaporitic minerals. The sequential precipitation of the Ca carbonates and Ca–Na carbonates (Fig. 3b,c) indicates progressive brine evaporation in Lonar waters. According to the model of evaporite formation (Hardie and Eugster, 1970), when the brines reach saturation the first minerals to

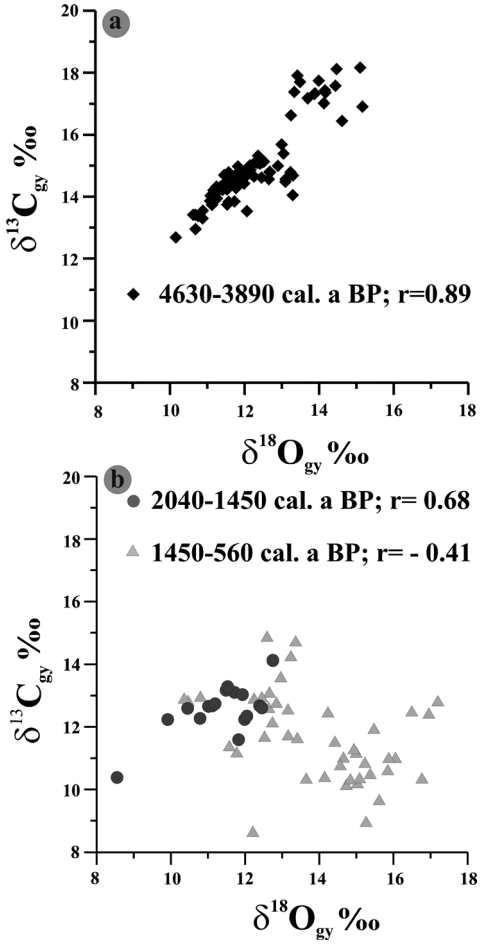

Figure 4. Covariance of $\delta^{13}C_{gy}$ and the $\delta^{18}O_{gy}$ isotope values from the lower (a) and upper (b) gaylussite zones.

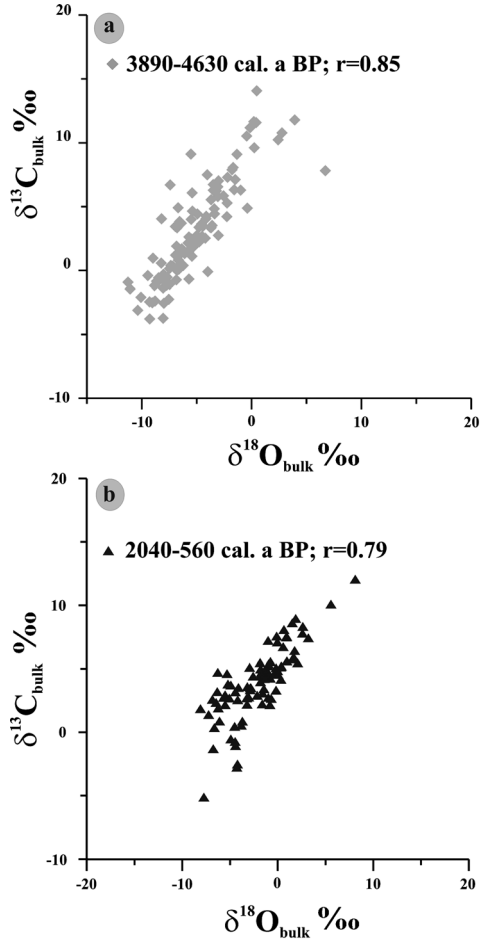

Figure 5. Covariance of $\delta^{13}C_{bulk}$ and the $\delta^{18}O_{bulk}$ isotope values from the lower (a) and upper (b) gaylussite zones.

precipitate are the alkaline earth carbonates (calcite and aragonite). The precipitation of these minerals continues until either Ca^{2+} or $CO_3{}^{2-}$ is exhausted. The selective removal of Ca induces a change in the ionic ratio of lake waters with a shift to a more Na-rich brine and results in precipitation of gaylussite. Interestingly, the trona crusts formed during the AD 1982 dry phase are not preserved in the core sediments, suggesting that dissolution of highly soluble evaporitic minerals also occurs in the basin.

We have also radiocarbon dated a single gaylussite crystal and a wood fragment from a depth of 266 cm, both of which yielded the same age of 1015 ± 35 cal a BP (Table 2), excluding any post-depositional alternation or diagenetic origin of gaylussite.

Possible factors influencing the formation of carbonates in Lonar: stream water chemistry and/or evaporation-induced salinity

A detailed understanding of the sources and chemistry of inflow into the Lonar Lake is essential to infer the processes governing evaporite formation. In addition to ephemeral runoff during the south-west monsoon, inflow into the lake is from three perennial streams (Dhara and Sitanahani in the north-east and Ramgaya in the east) (Fig. 1b). Tritium dating indicated a modern to sub-modern age for the groundwater. This is consistent with the local observations that a succession of below average rainfall results in partial or, as in AD 1982, a complete drying of the lake. As the stream inflow is closely linked to the monsoon rainfall, we consider the isotopic composition of stream water to be representative of local rainfall. Because Lonar is a closed basin the salinity changes can be assumed to be linked to input (inflow + precipitation)/evaporation ratio (I/E). The isotopic data from the inflowing streams and lake waters corroborate this assumption. The high $\delta^{18}O$ (+4.2 to +5.5‰) and δD (+14.7 to +21‰) values in lake waters compared with the inflowing streams ($\delta^{18}O = -2.1$ to -3.1‰, $\delta D = -15.4$ to -21.4‰) suggest evaporation from a closed system. A plot of $\delta^{18}O$ and δD isotope values along the Global Meteoric Water Line (GMWL) clearly supports the evaporative enrichment of lake water (Fig. 7). However, the high values of $\delta^{13}C_{DIC}$ (+12.9 to +14.8‰) can be induced both by loss of dissolved CO_2 due to strong evaporation, and by phytoplankton photosynthesis (Lei *et al.*, 2011). As the present-day Lonar Lake is observed to support luxuriant blooms of phytoplankton (Joshi *et al.*, 2008; our own observations between 2008 and 2011), the $\delta^{13}C_{DIC}$ enrichment in the lake waters cannot be interpreted in terms of evaporation processes alone.

The chemistry of lake and inflowing waters clearly indicates that Ca^{2+}, Mg^{2+} and K^+ are low (Table 1) in both lake waters and the inflowing streams. The decrease in Ca^{2+} in lake water compared with the inflowing streams is due to the continuous removal of Ca^{2+} by authigenic carbonate precipitation. However, the several orders of magnitude enrichment of sodium and chlorides in lake waters relative to the inflowing streams suggests that evaporation processes mainly control the water chemistry and seasonal stratification. The vertical variation of these ions with lake water depth, in combination with bottom anoxia, suggests evaporation-induced

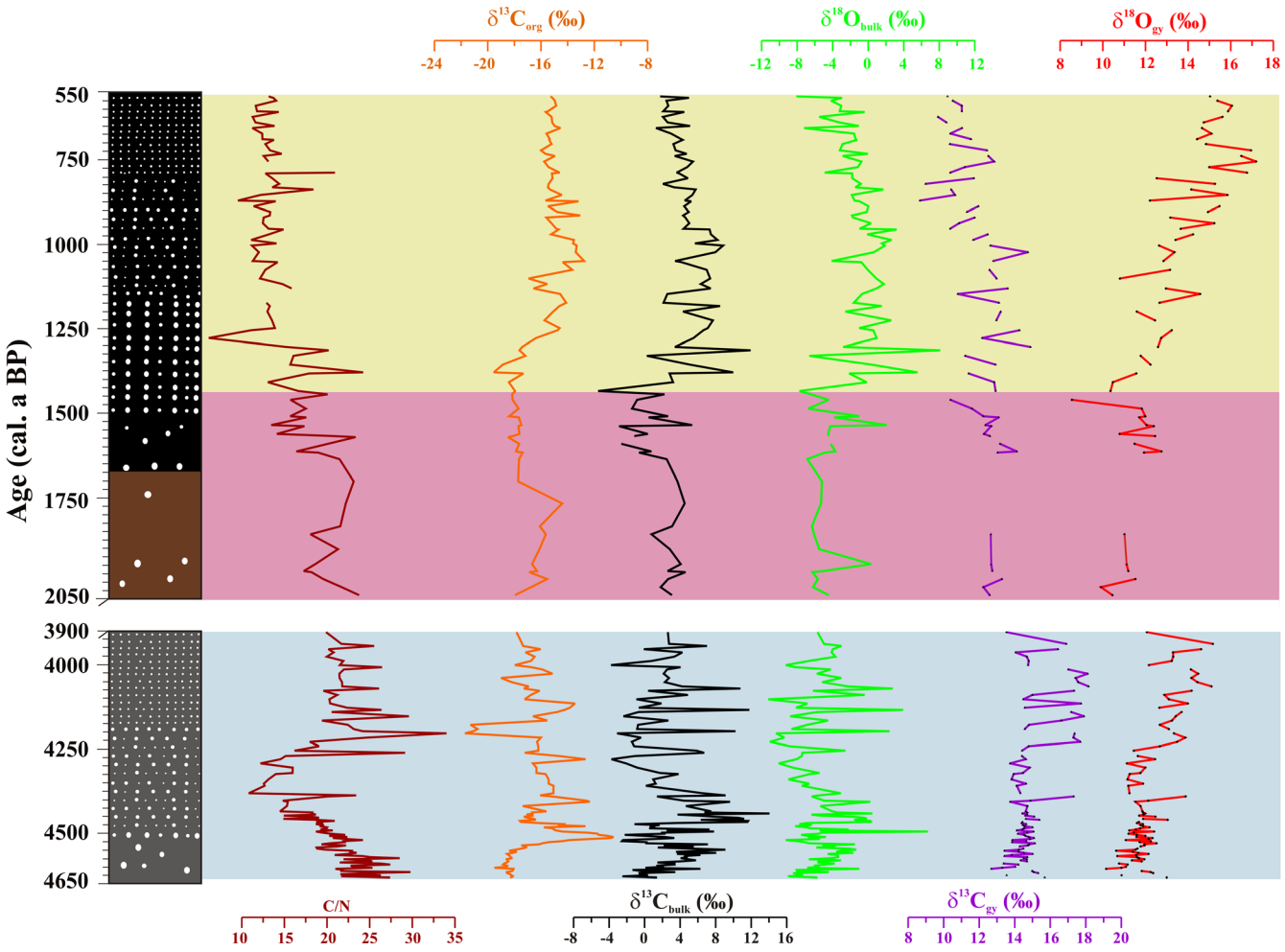

Figure 6. Isotope data on gaylussite crystals, bulk carbonates and organics ($\delta^{13}C_{org}$, C/N) from the gaylussite zones. (Color figure can be seen in the online version of this article, available at http://wileyonlinelibrary.com/journal/jqs)

stratification. In view of the minor contribution of Na (a major element in gaylussite) from the inflowing streams we conclude that the formation of gaylussite is controlled dominantly by salinity changes (I/E).

Modern (AD 1982) precipitation of trona during extremely saline conditions provides insights into the evaporative concentration processes resulting in the precipitation of carbonates. Trona crusts are formed due to complete dehydration by evaporation processes, resulting in the brine evolving into waters dominated by only a few major ions. The isotopically high values for the trona crystals (8.3 and 8.5‰ for $\delta^{18}O$ and 7.4 and 8‰ for $\delta^{13}C$) are typical of evaporite deposits.

Factors governing the isotopic composition of carbonates and organic matter

The oxygen isotopic composition of authigenic carbonate is controlled by (i) the isotopic composition of the water, (ii) temperature at the time of precipitation, (iii) potential evaporative enrichment and (iv) inflow (Talbot, 1990; Valero-Garcés *et al.*, 1999; Leng *et al.*, 2006). However, in hydrologically closed lakes, especially in non-karstic catchments, the enriched values are most likely to reflect preferential evaporative loss of the ^{16}O (Leng and Marshall, 2004).

The carbon isotopic composition of authigenic lacustrine carbonates is controlled by: (i) biological processes such as (a) methanogenesis – in eutrophic lakes anaerobic respiration of settling organic carbon produces biogenic methane and respired CO_2, which are characterized by significant depletion in ^{13}C (Hollander and Smith, 2001), and (b) photosynthesis, which selectively removes ^{12}C resulting in enrichment of ^{13}C in the DIC; (ii) variations in $^{13}C/^{12}C$ values of the dissolved inorganic carbon; and (iii) CO_2 exchange between water and atmosphere (Whiticar *et al.*, 1986; Talbot, 1990; Valero-Garcés *et al.*, 1999). Additionally, $\delta^{13}C$ enrichment in carbonates could also occur from the evaporation-induced loss of CO_2 from the brines (Stiller *et al.*, 1985; Rosen *et al.*, 1989; Mees *et al.*, 1998).

Several factors can influence the long-term ^{13}C record of the organic component in lake sediments. The dominant

Table 2. Radiocarbon dating of gaylussite crystals and a wood fragment from the same depth.

Sample no	Depth (cm)	Material	Lab. number	Age (^{14}C a BP) (1σ)	Age (cal. a BP) (1σ)
L17	266–266.5	Gaylussite crystal	Poz 41605	1105 ± 30	1015 ± 35
L16	266.5	Wood fragment	Poz 27190	1105 ± 30	1015 ± 35

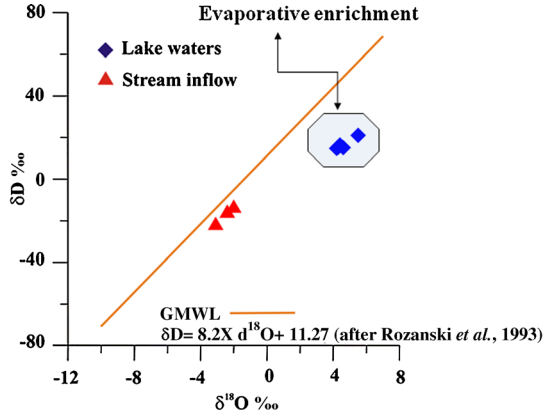

Figure 7. $\delta^{18}O$ and δD of the inflowing streams and lake water plotted along the Global Meteoric Water Line (GMWL). (Color figure can be seen in the online version of this article, available at http://wileyonlinelibrary.com/journal/jqs)

factors are changes in organic productivity and pH of the water (Stuiver, 1975). Photosynthesis associated with organic productivity preferentially uses ^{12}C, leaving the DIC pool enriched in ^{13}C (Goreau, 1977; Swart, 1983). Where dissolved CO_2 levels are low (<0.01 mol L^{-1}) photosynthetic organisms may be forced to change from CO_2 to HCO_3^- based metabolism. In some aquatic plants this becomes significant above pH 6.3 and is probably of considerable importance above pH 8.5. Assimilation of HCO_3^- can produce organic matter that is relatively enriched in ^{13}C (Talbot, 1990; Meyers, 1997; Leng and Marshall, 2004). These effects are important in an alkaline water body such as Lonar Lake. The net result will be an increase of $\delta^{13}C$ of the organic matter (Schelske and Hodell, 1991; Xu *et al.*, 2006).

Lower gaylussite zone (G1: 4630–3890 cal a BP)

The isotopic data must be interpreted bearing in mind that the calcite and aragonite are formed in surface waters while gaylussite is formed at the sediment–water interface. In the discussion below we explore the factors influencing the isotopic composition of bulk carbonates, gaylussite and organic matter, and their possible interlinkages.

Organic matter. The $\delta^{13}C_{org}$ value of organic matter is on average depleted by -31 and -20‰ compared with the $\delta^{13}C_{gy}$ of gaylussite crystals and the $\delta^{13}C_{bulk}$ of bulk carbonates, respectively. This is related to both the strong isotopic effect of carbon assimilation of up to -20‰ (Deuser *et al.*, 1968) and to the addition of isotopically even more depleted land plants and organic matter from soils. Even under the present highly eutrophic conditions, between 35 and 75% of the organic matter deposited in the Lonar Lake is derived from land plants (our unpublished data). Fluctuations in gaylussite carbon and oxygen isotopic ratios seem to be driven by evaporative cycles, whereas the $\delta^{13}C_{org}$ values are driven by differences in the input of land plants. C/N ratios in G1 zone with values >20 indicate a strong input from land plants. Between about 4450 and 4300 cal a BP the C/N ratios drop to values of ≤ 15, typical of planktonic organic matter (Meyers and Lallier-Verges, 1999), which may indicate enhanced productivity of the lake or reduced supply of terrestrial organic matter due to the dryer conditions. Above this sequence C/N values increase again and a peak at 4200 cal a BP is associated with minimum values in $\delta^{13}C_{org}$. As this occurs during the cycle of continuous evaporation we suspect that continuously dropping lake levels have led to stronger supply to terrestrial organic matter to the site.

Bulk carbonates. As gaylussite crystals were separated before analyses, the bulk isotope signal is contributed by the calcite and/or aragonite. It has already been shown that $\delta^{18}O$ of aragonite is about 0.6‰ more positive than calcite formed under the same conditions (Land, 1980; Leng and Marshal, 2004). However, the high correlation (0.85) shown by the $\delta^{18}O_{bulk}$ and $\delta^{13}C_{bulk}$ in this zone indicates that, as in the case of gaylussite, the isotopic enrichment of the bulk carbonate is controlled by evaporation processes.

Gaylussite crystals. The $\delta^{13}C_{gy}$ and $\delta^{18}O_{gy}$ of gaylussite crystals in the G1 zone show high values similar to the modern-day trona precipitated during extreme salinity conditions. The progressive enrichment of $\delta^{18}O_{gy}$ observed in gaylussite crystals can be attributed to lake waters that have undergone systematic evaporation (Craig and Gordon, 1965; Gibson *et al.*, 1993). The high correlation between carbon and oxygen isotopes is characteristic of hydrologically closed lakes (Talbot, 1990; Li and Ku, 1997). We conclude that the co-varying high value ($r = 0.89$) for $\delta^{18}O_{gy}$ and $\delta^{13}C_{gy}$ in gaylussite is a result of evaporative processes.

Upper gaylussite zone (G2: 2040–560 cal a BP)

Organic matter. The $\delta^{13}C_{org}$ and C/N values in the lower part (2040–1450 cal a BP) in the G2 zone show similarity to the G1 zone, indicating a contribution derived from land plants. However, the sudden persistent shift to high values for $\delta^{13}C_{org}$ and lowering trend in C/N in the upper part (1450–550 cal a BP) indicates dominance of aquatic productivity in the lake.

Bulk carbonates. The high correlation between $\delta^{18}O_{bulk}$ and $\delta^{13}C_{bulk}$ (0.79) indicates, as in the lower part (G1), evaporation-induced precipitation from a closed basin. There is high enrichment in bulk carbonate values around ca. 1450 cal a BP followed by stable values until 550 cal a BP.

Gaylussite. This section can be divided into two parts: a lower part (ca. 2040–1450 cal a BP) where the high $\delta^{18}O$ and $\delta^{13}C$ values of gaylussite crystals and their high positive correlation (0.68) indicates evaporation as the major control on both stable isotopic ratios. There is a decoupling of $\delta^{13}C_{gy}$ and $\delta^{18}O_{gy}$ of gaylussite beginning ca. 1450 cal a BP when $\delta^{18}O_{gy}$ continues to show progressive enrichment and $\delta^{13}C_{gy}$ remains stable or shows depletion. The depletion in $\delta^{13}C_{gy}$ of gaylussite crystals parallels a shift of C/N to planktonic values (≤ 15), indicating eutrophication in the lake.

However, high primary productivity in lakes should result in high $\delta^{13}C$ in the organic matter, bulk carbonates and gaylussite crystals, which is not seen in our data where $\delta^{13}C_{gy}$ shows a depleting trend beginning ca. 1450 cal a BP. An explanation comes from the fact that the gaylussite, unlike calcite and aragonite, forms at the sediment–water interface and, under persistent, well-stratified conditions, could incorporate the ^{12}C released by organic matter remineralization and methanogenesis (Drummond *et al.*, 1995; Hollander and Smith, 2001) (Fig. 8). Thus, decoupling of ^{18}O and ^{13}C in gaylussite ca. 1450 cal a BP, which intensifies ca. 1000 cal a BP, suggests persistent stratification, with anoxia and methanogenesis in the hypolimnion as observed in stratified eutrophic lakes (Hollander and Smith, 2001).

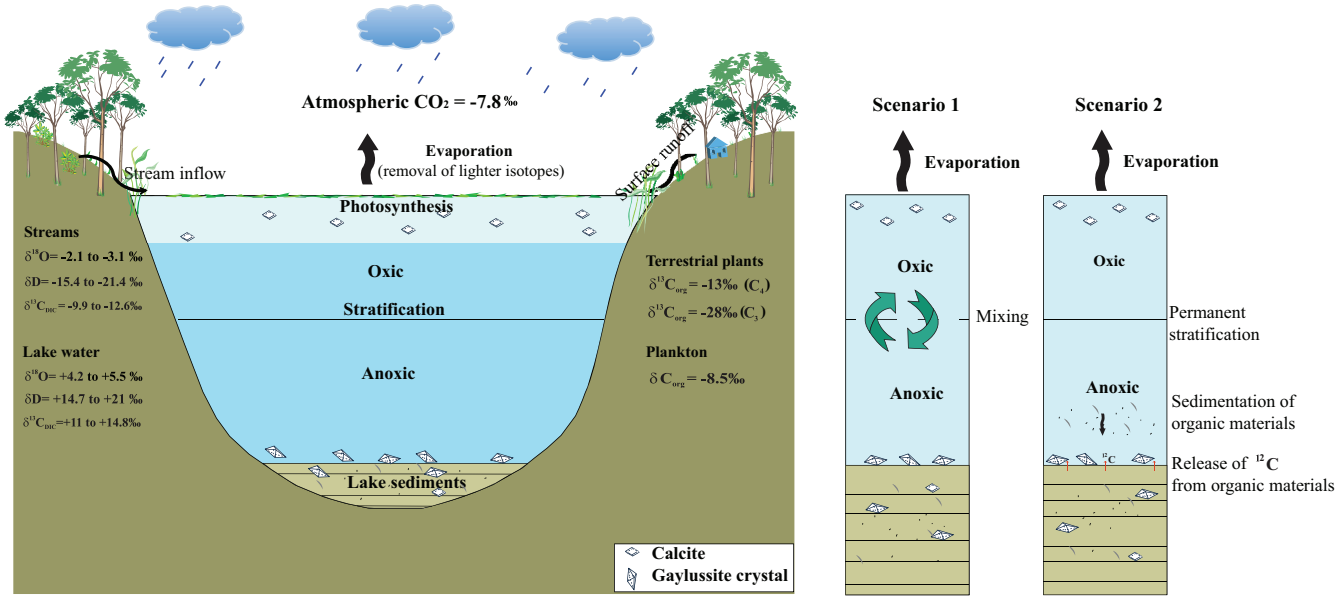

Figure 8. Schematic representation of the processes determining the $\delta^{13}C$ and the $\delta^{18}O$ in lake sediments and evaporites (calcite/aragonite and gaylussite). (Color figure can be seen in the online version of this article, available at http://wileyonlinelibrary.com/journal/jqs)

Do isotopes of gaylussite offer any additional environmental information compared with isotope data from calcite and/or aragonite?

The environmental implications of the occurrence of primary gaylussite, a palaeosalinity indicator, are evident. In the case of Lonar Lake sediments, the isotopic information obtained from gaylussite largely corroborates inferences from bulk carbonates (calcite and/or aragonite). It is only in the upper gaylussite zone (G2) that the additional benefit of isotopic analyses of gaylussite becomes clear; here the $\delta^{13}C_{gy}$ indicates persistent stratification in lake waters and occurrence of methanogenesis between 1450 and 560 cal a BP.

Palaeoclimatic significance of evaporative gaylussite crystals

Using mineralogical and isotope analyses we can, for the first time, identify two persistent centennial-scale droughts (4630–3890 cal a BP and 2040–560 cal a BP) in the CMZ. The onset of the first drought (4630–3890 cal a BP) is also marked by the final drying of lakes in arid north-west India, and by a weaker monsoon in other regions of southern, central and northern-eastern India, the north-west Himalaya, and eastern Tibet (Rajagopalan *et al.*, 1997; Hong *et al.*, 2003; Prasad and Enzel, 2006; Demske *et al.*, 2009; Rashid *et al.*, 2011; Dixit and Bera, 2012; Quamar and Chauhan, 2012; Ponton *et al.*, 2012). The second drier period in the Lonar Lake (2040–560 cal a BP) encompasses the so called Medieval Warming Period (MWP) in Europe (1300–900 AD; Mann and Jones, 2003) but this change began much earlier in the Lonar Lake. Pollen sequences in north-eastern India also indicate dry conditions between 2000 and 1000 cal a BP followed by a wetter interval from 1000 to 400 cal a BP (Mazari *et al.*, 1996, in Denniston *et al.*, 2000). The drying trend observed in Lonar Lake is opposite to that reported from the Dandak cave stalagmites where stronger monsoon rainfall has been reported (ca. 1340–910 AD; Sinha *et al.*, 2007) or even with the upwelling record from the Arabian Sea (Gupta *et al.*, 2003), indicating considerable spatial inhomogeneity in ISM precipitation during the late Holocene.

Conclusion

Detailed geochemical investigations were carried out on bulk carbonates, organic matter and gaylussite crystals from the lacustrine sediments in Lonar Lake, central India, over selected intervals (4630–3890 and 2040–560 cal a BP). Results from analyses of modern hydrochemistry and lake water isotopes ($\delta^{18}O$ and δD) show that Lonar Lake responds to I/E ratio. The sedimentological and mineralogical evidence from the core sediments indicates evaporation with a progressive enrichment of brine resulting in the precipitation of gaylussite crystals. Isotopic analysis ($\delta^{18}O_{gy}$ and $\delta^{13}C_{gy}$) of gaylussite crystals shows strong enrichment typical of evaporite deposits. The high covariance between $\delta^{18}O$ and $\delta^{13}C$ on the evaporative gaylussite crystals and residual bulk carbonates (calcite) from the long core reveals evaporation as a major controlling factor for isotopic enrichment. The lack of covariance between $\delta^{18}O_{gy}$ and $\delta^{13}C_{gy}$ for gaylussite crystals from ca. 1450 to 560 cal a BP indicates persistent stratification and onset of methanogenesis in the lake.

Acknowledgements. This project was funded by the Deutsche-forschungsgemeinschaft under the coordinated programme 'Himalaya: Modern and Past Climates' (HIMPAC, FOR 1380). The Lonar coring and field expeditions received financial and logistic support from the Deutsches GFZ Potsdam, Indian Institute of Geomagnetism and the Universität Potsdam. Water sample analyses and tritium dating were undertaken at the UFZ Helmholtz Centre for Environmental Research. Thanks are due to R. Niederreiter for coring, S. Pinkerneil and L. Czudowski for their help in preparing the samples. The cooperation of the Forest and Wildlife Department of Maharashtra State (India) is gratefully acknowledged.

Abbreviations. CMZ, core monsoon zone; GMWL, Global Meteoric Water Line; I/E, input (inflow + precipitation)/evaporation ratio; ISM, Indian summer monsoon; MWP, Medieval Warming Period; P/E, precipitation/evaporation ratio; XRD, X-ray diffraction; XRF, X-ray fluorescence

References

Ashok K, Guan Z, Saji NH, *et al.* 2004. On the individual and combined influence of the ENSO and the Indian Ocean Dipole on the Indian Summer Monsoon. *Journal of Climate* **17**: 3141–3154.

Badve RM, Kumaran KPN, Rajshekhar C. 1993. Eutrophication of Lonar Lake, Maharashtra. *Current Science* **65**: 347–351.

Borul SB. 2012. Study of water quality of Lonar Lake. *Journal of Chemical and Pharmaceutical Research* **4**: 1716–1718.

Bischoff JL, Herbst DB, Rosenbauer RJ. 1991. Gaylussite formation at Mono Lake, California, USA. *Geochim Cosmochim Acta* **55**: 1743–1747.

Bronk Ramsay C. 2008. Deposition models for chronological records. *Quaternary Science Reviews* **27**: 42–60.

Bronk Ramsay C. 2009. Bayesian analysis of radiocarbon dates. *Radiocarbon* **51**: 337–360.

Buchardt B, Israelson C, Seaman P, *et al*. 2001. Ikaite tufa towers in Ikka Fjord, Southwest Greenland: their formation by mixing of seawater and alkaline spring water. *J Sedimentary Res* **71**: 176–189.

Chakrabarti R, Basu AR. 2006. Trace element and isotopic evidence for Archean basement in the Lonar crater impact breccia, Deccan Volcanic Province. *Earth and Planetary Science Letters* **247**: 197–211.

Craig H, Gordon LI. 1965. Deuterium and oxygen-18 variations in the ocean and the marine atmosphere. In *Proceedings of the 1965 Conference on Stable Isotopes in Oceanographic Studies and Paleotemperatures (held at Spoleto, Italy)*, Tongiorgi E (ed.). V. Lishi e F., Pisa, Italy; 9–130.

Demske D, Tarasov PE, Wünnemann B, *et al*. 2009. Late glacial and Holocene vegetation, Indian monsoon and westerly circulation in the Trans-Himalaya recorded in the lacustrine pollen sequence from TsoKar, Ladakh, NW India. *Palaeogeography, Palaeoclimatology, Palaeoecology* **279**: 172–185.

Denniston RF, Asmerom Y, Sharma RH, *et al*. 2000. Speleothem evidence for changes in Indian summer monsoon precipitation over the last ~2300 years. *Quaternary Research* **53**: 196–202.

Deuser EG, Degens ET, Guillard RRL. 1968. Carbon isotope relationships between plankton and seawater. *Geochimica et Cosmochimica Acta* **32**: 657–660.

Dixit S, Bera SK. 2012. Holocene climatic fluctuations from Lower Brahmaputra flood plain of Assam. *northeast India. J. Earth Syst. Sci.* **121**: 135–147.

Drummond CN, Patterson WP, Walker JC. 1995. Climate forcing of carbon–oxygen isotopic covariance in temperate-region marl lakes. *Geology* **23**: 1031–1034.

Eugster HP, Hardie LA. 1978. Saline lakes. In *Lakes: Chemistry, Geology, Physics, Saline lakes*, Lerman A (ed.). Springer: New York; 237–293.

Fredriksson K, Dube A, Milton DJ, *et al*. 1973. Lonar Lake, India: an impact crater in basalt. *Science* **180**: 862–864.

Fudali RF, Milton DJ, Fredriksson K, *et al*. 1980. Morphology of Lonar crater, India: comparisons and implications. *The Moon and the Planets* **23**: 439–515.

Gadgil S. 2003. The Indian Monsoon and its variability. *Annual Review Earth Planet. Sci.* **31**: 429–467.

Gibson JJ, Edwards TWD, Bursey GG, *et al*. 1993. Estimating evaporation using stable isotopes: quantitative results and sensitivity analysis for two catchments in northern Canada. *Nordic Hydrology* **24**: 79–94.

Goreau TJ. 1977. Seasonal variations of trace metals and stable isotopes in coral skeleton: physiological and environmental controls. *Proc 3rd Int Coral Reef Symp* **2**: 425–430.

Gupta AK, Anderson DM, Overpeck JT. 2003. Abrupt changes in the Asian southwest monsoon during the Holocene and their links to the North Atlantic Ocean. *Nature* **421**: 354–357.

Hardie LA, Eugster HP. 1970. The evolution of closed-basin brines. In 50th Anniversary Symposia: Mineralogy and Petrology of the Upper Mantle; Sulfides; Mineralogy and Geochemistry of Non-Marine Evaporites, Morgan BA (ed.). *Min. Soc. Am Spec. Paper No.* **3**: 273–290.

Hollander DJ, Smith MJ. 2001. Microbially mediated carbon cycling as a control of the $\delta^{13}C$ of sedimentary carbon in eutrophic Lake Mendota (USA): new models for isotopic excursions in the sedimentary record. *Geochim. Cosmochim. Acta* **65**: 4321–4337.

Hong YT, Hong B, Lin QH, *et al*. 2003. Correlation between Indian Ocean summer monsoon and North Atlantic climate during the Holocene. *Earth and Planetary Science Letters* **211**: 371–380.

Jhingran AG, Rao KV. 1958. Lonar Lake and its salinity. *Records of the Geological Survey of India* **85**: 313–334.

Joshi AA, Kanekar PP, Kelkar AS, *et al*. 2008. Cultivable bacterial diversity of alkaline Lonar Lake, India. *Microb. Ecol.* **55**: 163–172.

Jourdan FF, Moynier F, Koeberl C, *et al*. 2011. $^{40}AR/^{39}AR$ age of the Lonar crater and consequence for the geochronology of planetary impacts. *Geology* **39**: 671–674.

Krishnan R, Zhang C, Sugi M. 2000. Dynamics of breaks in the Indian summer monsoon. *Journal of Atmospheric Sciences* **57**: 1354–1372.

Land LS. 1980. The isotopic and trace element geochemistry of dolomite: the state of the art. In Concepts and Models of Dolomitization, Zenger DH, Dunham JB, Ethington RL (eds). *SEPM Spec. Publ.* **28**: 87–110.

La Touche THD, Christie WAK. 1912. The geology of the Lonar Lake. With a note on the Lonar soda deposit by Christie WAK. *Rec. Geol. Surv. India* **36**: 235–263.

Lei Y, Yao T, Sheng Y, *et al*. 2011. Characteristics of $\delta\ ^{13}C_{DIC}$ in lakes on the Tibetan Plateau and its implications for the carbon cycle. *Hydrological Processes* **26**: 535–543.

Leng MJ, Lamb AL, Heaton THE, *et al*. 2006. Isotopes in lake sediments. In *Isotopes in Palaeoenvironmental Research*, Leng MJ (ed.). Springer: Dordrecht; 147–184.

Leng MJ, Marshall JD. 2004. Palaeoclimate interpretation of stable isotope data from lake sediment archives. *Quaternary Science Reviews* **23**: 811–831.

Li HC, Ku TL. 1997. $\delta^{13}C - \delta^{18}O$ covariance as a paleohydrological indicator for closed basin lakes. *Palaeogeography, Palaeoclimatology, Palaeoecology* **133**: 69–80.

Maloof AC, Stewart ST, Weiss BP, *et al*. 2009. Geology of Lonar Crater, India. *GSA Bulletin* **122**: 109–126.

Mangili C, Plessen B, Wolff C, *et al*. 2010. Climatic implications of annual to decadal resolution stable isotope data from calcite varves of the Piànico interglacial lake record, Southern Alps. *Global and Planetary Change* **71**: 168–174.

Mann ME, Jones PD. 2003. Global surface temperatures over the past two millennia. *Geophysical Research Letters* **30**: 1820–1824.

Mazari RK, Bagati TN, Chauhan MS, *et al*. 1996. Palaeoclimatic record of last 2000 years in trans-Himalayan Lahaul-Spiti region. In Paleoclimate and Environmental Variability in Austral-Asian Transect during the Past 2000 Years. In *Proceedings, IGBP-PAGES/PEP II Symposium, on Paleoclimate and Environmental variability in the Austral-Asia Transect during the past 2000 Years. Nagoya University*, Japan, pp. 262–269.

McConnaughey TA, LaBaugh JW, Rosenberry DO, *et al*. 1994. Carbon budget for a groundwater-fed lake: calcification supports summer photosynthesis. *Limnol Oceanogr* **39**: 1319–1332.

Mees F, Reyes E, Keppens E. 1998. Stable isotope chemistry of gaylussite and nahcolite from the deposits of the crater lake at Malha, northern Sudan. *Chemical Geology* **146**: 87–98.

Mees F, Verschuren D, Nijs R, *et al*. 1991. Holocene evolution of the crater lake at Malha, Northwest Sudan. *Journal of Paleolimnology* **5**: 227–253.

Meyers PA, Lallier-Verges E. 1999. Lacustrine sedimentary organic matter records of late Quaternary paleoclimates. *Journal of Paleolimnology* **21**: 345–372.

Meyers PA. 1997. Organic geochemical proxies of palaeogeographic, paleolimnologic, and paleoclimatic processes. *Org. Geochem.* **27**: 213–250.

Milton DJ, Dube A, Sen Gupta SS. 1975. Deposition of ejecta at Lonar crater. *Meteoritics* **10**: 456–457.

Misra S, Arif Md, Basavaiah N, *et al*. 2010. Structural and anisotropy of magnetic susceptibility (AMS) evidence for oblique impact on terrestrial basalt flows: Lonar crater, India. *GSA Bulletin* **122**: 563–574.

Naidu AS, Murali AV, Mowatt TC. 1990. Preliminary mineral analysis of the clay fraction of the red bole beds, Deccan Traps, India. *EOS* **71**: 1713.

Nandy NC, Deo VB. 1961. Origin of the Lonar Lake and its alkalinity. *TISCO* **8**: 144–155.

Pendall EG, Harden JW, Trumbore SE, *et al*. 1994. Isotopic approach to soil carbonate dynamics and implications for paleoclimatic interpretations. *Quaternary Research* **42**: 60–71.

Partridge TC, Kerr SJ, Metcalfe SE, *et al*. 1993. The Pretoria Saltpan: a 200,000 year Southern African lacustrine sequence. *Palaeogeography, Palaeoclimatology, Palaeoecology* **101**: 317–337.

Pawar AL. 2010. Seasonal variation in physicochemical quality of Lonar Lake water. *Journal of Chemical and Pharmaceutical Research* **2**: 225–231.

Ponton C, Giosan L, Eglinton TI, *et al*. 2012. Holocene aridification of India. *Geophys. Res. Lett.*, **39**: 1–6.

Prasad S, Negendank JFW. 2004. Holocene palaeoclimate in the Saharo-Arabian Desert. In *The Climate in Historical Times: Towards a Synthesis of Holocene Proxy Data and Climate Models*, Fischer H, Kumke T, Lohmann G, Flöser G, Miller H, von Storch H, Negendank JFW (eds). Springer: Berlin; 209–228.

Prasad S, Enzel Y. 2006. Holocene paleoclimates of India. *Quaternary Research* **66**: 442–453.

Quamar MF, Chauhan MS. 2012. Late Quaternary vegetation, climate as well as lake-level changes and human occupation from Nitaya area in Hoshangabad District, southwestern Madhya Pradesh (India), based on pollen evidence. *Quaternary International* **263**: 104–113.

Rajagopalan G, Sukumar R, Ramesh R, *et al*. 1997. Late Quaternary vegetational and climatic changes from tropical peats in southern India – an extended record up to 40,000 years BP. *Current Science* **73**: 60–63.

Rajeevan MS, Gadgil S, Bhate J. 2010. Active and break spells of the Indian summer monsoon. *J. Earth Syst. Sci.* **119**: 229–247.

Rankama K, Sahama TG. 1964. *Geochemistry*. University of Chicago Press: Chicago.

Rashid H, England E, Thompson L, *et al*. 2011. Late glacial to Holocene Indian summer monsoon variability based upon sediment records taken from the Bay of Bengal. *Terr. Atmos. Ocean. Sci.*, **22**: 215–228.

Reddy MM, Hoch A. 2011. Calcium carbonate nucleation in alkaline lake surface water, Pyramid Lake, Nevada, USA. *Aquatic Geochemistry* **18**: 95–113.

Reimer PJ, Baillie MGL, Bard E, *et al*. 2009. IntCal09 and Marine09 radiocarbon age calibration curves, 0–50,000 years cal BP. *Radiocarbon* **51**: 1111–1150.

Renaut RW, Tiercelin JJ, Owen RB. 1986. Mineral precipitation and diagenesis in the sediments of the Lake Bogoria basin, Kenya Rift Valley. In Sedimentation in the African Rifts, Frostick LE, Renaut RW, Reid I, Tiercelin JJ (eds), *Spec. Publ. Geol. Soc. Lond.* **25:** 159–175.

Rosen MR, Miser DE, Starcher MA, *et al*. 1989. Formation of dolomite in the Coorong region, South Australia. *Geochim. Cosmochim. Acta* **53**: 661–669.

Rozanski K, Araguas-Araguas L, Gonfiantini R. 1993. Isotopic patterns in modern global precipitation. In Climate Change in Continental Isotopic Record, Swart PK, Lohman, KL, McKenzie JA, Savin S (eds), *Geophysical Monograph* **78:** 1–37.

Schelske CL, Hodell DA. 1991. Recent changes in productivity and climate of Lake Ontario detected by isotope analysis of sediments. *Limnol. Oceanogr.* **36**: 961–975.

Sengupta S, Sarkar A. 2006. Stable isotope evidence of dual (Arabian and Bay of Bengal) vapour sources in monsoonal precipitation over north India. *Earth Planet. Sci. Lett.*, **250**: 511–521.

Sinha A, Cannariato KG, Stott LD, *et al*. 2007. A 900-year (600 to 1500 A.D.) record of the Indian summer monsoon precipitation from the core monsoon zone of India. *Geophysical Research Letters* **34**: L16707.

Spötl C, Nicolussi K, Patzelt G, *et al*. 2010. Humid climate during deposition of sapropel 1 in the Mediterranean Sea: assessing the influence on the Alps. *Global and Planetary Change* **71**: 242–248.

Spötl C, Vennemann TW. 2003. Continuous-flow IRMS analysis of carbonate minerals. *Rapid Communications in Mass Spectrometry* **17**: 1004–1006.

Stiller M, Rounick JS, Shasha S. 1985. Extreme carbon-isotope enrichments in evaporating brines. *Nature* **316**: 434–435.

Stuiver M. 1970. Oxygen and carbon isotope ratios of freshwater carbonates as climatic indicators. *J. Geophys. Res.* **75**: 5247–5257.

Stuiver M. 1975. Climate versus changes in ^{13}C content of the organic component of lake sediments during the late Quarternary. *Quaternary Research* **5**: 251–262.

Swart PK. 1983. Carbon and oxygen isotope fractionation in scleractinian corals: a review. *Earth-Sci Rev* **19**: 51–80.

Talbot MR. 1990. A review of the palaeohydrological interpretation of carbon and oxygen isotopic ratios in primary lacustrine carbonates. *Chemical Geology (Isotope Geoscience Section)* **80**: 261–279.

Valero-Garcés BL, Delgado-Huertas A, Ratto N, *et al*. 1999. Large ^{13}C enrichment in primary carbonates from Andean Altiplano lakes, northwest Argentina. *Earth and Planetary Science Letters* **171**: 236–266.

Whiticar MJ, Faber E, Schoell M. 1986. Biogenic methane formation in marine and freshwater environments: CO_2 reduction vs. acetate fermentation—Isotopic evidence. *Geochim. Cosmochim. Acta* **50**: 693–709.

Xu H, Ai L, Tan L, *et al*. 2006. Stable isotopes in bulk carbonates and organic matter in recent sediments of Lake Qinghai and their climatic implications. *Chemical Geology* **235**: 262–275.